11 WCEE

Copyright © 1996 Elsevier Science Ltd
Paper No. 754. (quote when citing this article)
Eleventh World Conference on Earthquake Engineering
ISBN: 0 08 042822 3

NONLINEAR FINITE ELEMENT ANALYSIS OF CONFINED MASONRY WALLS

K. ISHIBASHI
Department of Architecture, Chiba Institute of Technology
2-17-1 Tsudanuma Narashino-City, Chiba, 275 Japan

H. KATSUMATA, K. NAGANUMA, M. OHKUBO
Technical Research Institute of Obayashi Corporation
4-640 Shimkiyoto Kiyose-City, Tokyo, 204 Japan

ABSTRACT

Structural experiments of five confined masonry wall specimens had already been done at CENAPRED (the national center for earthquake disaster prevention) in Mexico city,in order to investigate behavior of a brick wall surrounded by a reinforced concrete frame under earthquake condition. A lot of data on failure modes and strengths had been obtained from the experiments (Ishibashi *et al.*, 1992), but the data did not sufficiently clarify the behavior of masonry walls during earthquake. This paper discusses most dominant elements and their constitutive law to analyze a confined masonry brick wall. An element on boundary between a brick wall and a concrete column, called "bonding element", was found to give stronger effects on failure modes and lateral loads-displacement relationship at the time when it was applied on nonlinear finite element analysis using a supercomputer. A constitutive law of the bonding element based on a series of tests showing relation between shear and slip displacement is proposed and a rational explanation of behavior of confined masonry structure is made.

KEY WORDS

Brick wall; confined masonry; wall reinforcement; structural experiments; lateral load; vertical load; cyclic loading; finite element method; joint element; supercomputer.

SPECIMENS OF TESTS

Specimen WBW was produced as a standard specimen in which two walls were connected by a beam and a slab. In the case of specimen W-W two walls were connected by tension lods. Specimen WWW had spandrels added to the standard specimen WBW. Specimen WBW-E was reinforced in walls by horizontal reinforcements (ladder-shaped steel bars) in every two layers of brick (reinforcement ratio is 0.089%). Specimen WBW-B was reinforced by horizontal deformed steel bars in every three layers of brick (reinforcement ratio is 0.089%).

DISTRIBUTION OF FINITE ELEMENTS TO ANALYSIS MODELS

Loading forces and meshed finite elements for specimen WBW is shown in Fig. 1. The plane stress condition was assumed in the analyses based on the shapes of the specimens and the loading conditions. It is considered that the effects of the foundation slab on the behavior of the specimen would be negligible, so all the specimens were fixed completely at the top of the foundation slab. Four-node quadrilateral plane stress elements were used for modeling the brick wall, the surrounding reinforced concrete frame and the foundation slab. The brick wall was modeled as a material having uniform characteristics (from test of masonry pile) because an enormous number of elements would be needed to model the bricks and the joints individually. The element size was almost equal to two layers of brick in the vertical direction because some specimens have horizontal reinforcing bars in every other brick layer. Since truss elements were used for modeling those bars, nodes were generated corresponding to the reinforcing bar locations. The mesh in the vertical direction is selected to make the elements as square as possible. The size of the elements was identical for all specimens. Equivalent reinforcement layers with stiffness in only one direction were substituted for the longitudinal bars and the shear reinforcements in the surrounding reinforced concrete frame, and those layers were superimposed on the plane stress elements. The reinforcing bars in the walls were replaced by truss element, and arranged at corresponding positions in the masonry walls. As for specimen WBW–B, truss elements with equivalent sections having the same amount of reinforcing bars in the walls were used because the mesh lines did not correspond to the reinforcing bars. The horizontal joints in the brick wall were almost three times as srong as the brick. Thus they were replaced by equivalent two–node spring elements and distributed along the entire element mesh line in the horizontal direction of the brick wall. With the increased load, separation and slippage might be anticipated along the boundary surface between the brick wall and the surrounding reinforced concrete frame. In order to simulate this behavior, the brick wall and the surrounding frame were connected by two–node linkage elements of two orthogonal springs. Axial loads were applied to three nodes at each loading point and the horizontal load was applied to two nodes corresponding to the loading points in the experiment.

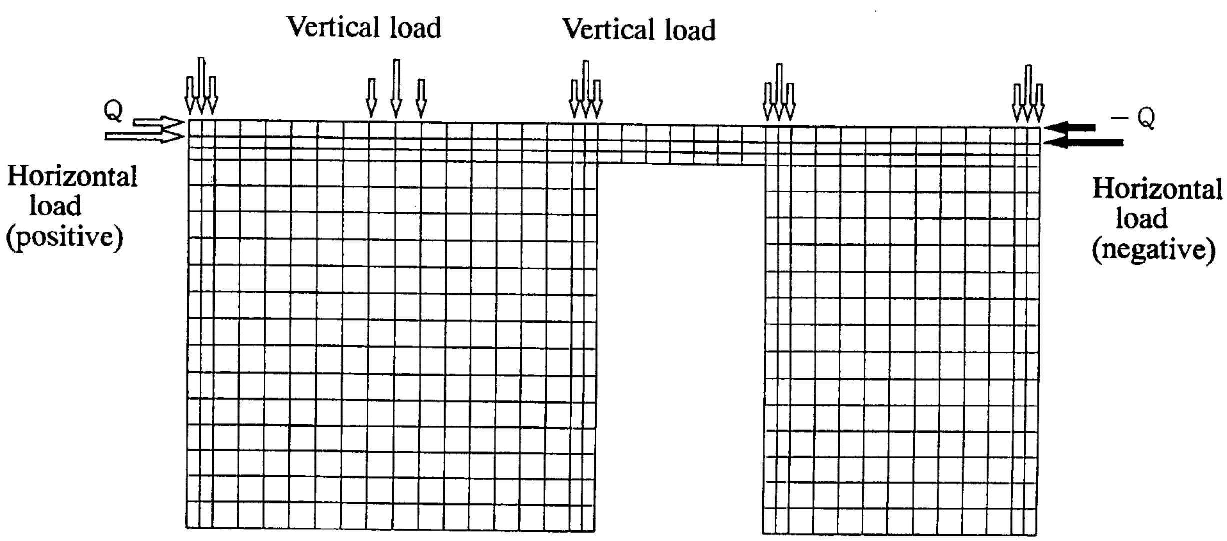

Fig. 1 Loading forces and meshed finite elements for specimens

MODELING OF MATERIAL CHARACTERISTICS

Material properties of the masonry pile, concrete, joint mortar and reinfrcing bars were based on the corresponding material test results. The constitutive law of concrete under plane stress condition was based on the orthotropic model with the concept of equivalent uniaxial strain proposed by Darwin *et al.* (1977) and the failure criteria under biaxial stress condition followed the equation proposed by Kupfer *et al.* (1973). The stress–strain relationship of concrete was expressed by linear elasticity up to the occurrence of cracking on the tension side, and by the exponential function curve proposed by Fafitis *et al.* (1985) in the compression side. The occurrence of cracking was judged on the basis of the principal stress criteria, and after cracking, the stress and stiffness in the direction normal to the crack were considered to be zero. The masonry pile was treated in the same manner as concrete.

With regard to the characteristics of linkage elements inserted between the masonry pile and the surrounding frame, normal stiffness on the boundary surface was large enough and assumed to have linear elasticity cut by the tensile strength of the masonry pile in the tension zone as shown in Fig. 2(a). Characteristics in the shear direction were modeled considering the effects of acting normal stress referring to the results of direct shear tests of brick joints (Fujii *et al.*, 1990). Namely, as shown in Fig. 2(b), the relationship between shear stress and shear slip is expressed by a bilinear model, and the stress of the first turning point is successively increased by 0.8 times of the acting normal compressive stress. This corresponds to the assumption that the friction coefficient at the boundary surface is equal to 0.8. The shear stress at the first turning point(τ_1) was defined based on the diagonal compression tests of masonry piles. The following relationships could be written for the shear stress (τ_u) and normal stress (σ_n; compression is positive) acting on the joint at the point of failure from the loading condition since shear slip failure had occurred in the diagonal compression tests of masonry piles.

$$\tau_u = \sigma_n \tag{1}$$

Assuming the friction coefficient to be 0.8, the following equation is obtained.

$$\tau_u = \tau_1 + 0.8\,\sigma_n \quad \text{(when } \sigma_n \text{ is compression)} \tag{2}$$

Substituting Eq.(1) for Eq.(2), then,

$$\tau_1 = 0.2\,\sigma_n \tag{3}$$

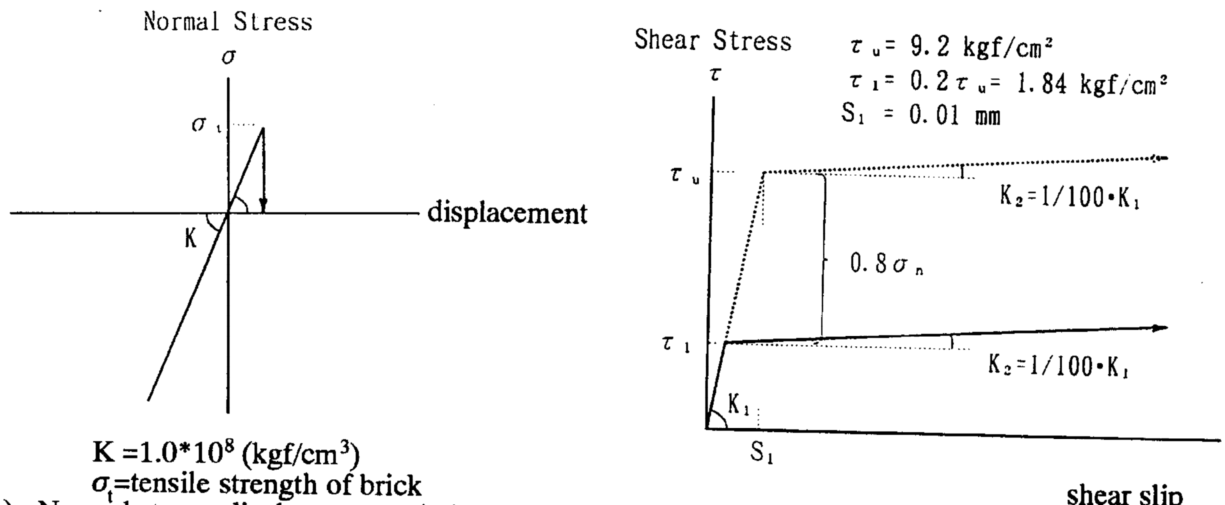

(a) Normal stress–displacement relationship (b) Shear stress–shear slip relationship

Fig. 2 Characteristics of linkage elements on the boundary surface between a brick wall and a suronding concrete frame

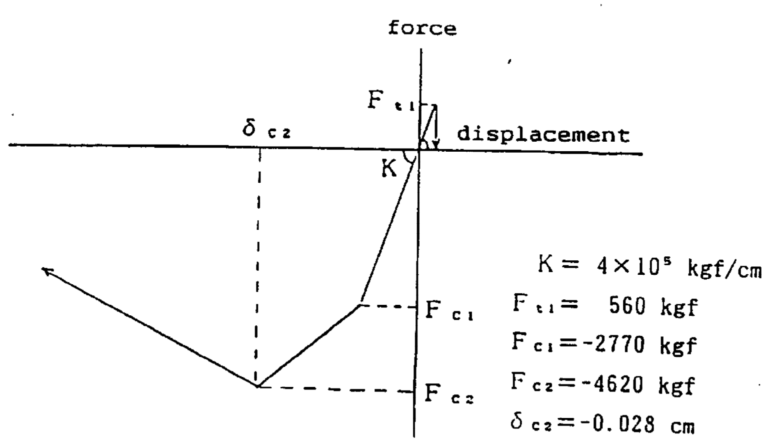

Fig. 3 Characteristics of spring elements for joint mortar in a brick wall

In case the normal stress σ_n is tensile, σ_n in Eq.(1) is to be zero. After the normal stress reaches the tensile strength of brick, stiffness in the shear direction is set to zero. Thus characteristics of the spring elements were determined in an asymmetrical form in the tension and compression zone as shown in Fig. 3 so as to correspond to the material properties of the joint mortar.

ANALYSIS CASES AND RESULTS

Five specimens in total of 19 cases were analyzed. Analysis cases and their parameters and results are listed in Table 1. Major parameters are loading directions (positive, or negative) and magnitude of the vertical load (standard, standard ±20%). Among the cases included is one for investigating the effects of the restraining force in tension rods connecting both top sides of the specimen during the early stages of the test of specimen W–W (Case 7). In other cases horizontal loads were first applied to a certain extent (20tf),then reloading in the opposite direction up to the point of failure (Cases 18 and 19). These cases are

Table 1. Analysis cases and parameters and results

Case	Specimen	Parameters: Horizonta load	Parameters: Vertical load	Analysis conditions	Results of maximum loads: Test(tf) (Deformation Angle 10^{-3}rad.)	Analysis(tf)	Ratio
1	WBW	Positive	Standard	One-way	26.4(1.35)	24.8(1.59)	1.06
2		Negative			25.5(1.53)	24.0(1.12)	1.06
3		Positive	Standard+20%		----	26.8(1.98)	----
4			Standard−20%		----	23.3(1.47)	----
5	W−W	Positive	Standard	One-way	22.2(1.38)	23.2(1.33)	0.96
6		Negative	Standard		24.0(1.57)	23.1(1.54)	1.04
7		Positive	Standard	With restraining force of tension rods	22.2(1.38)	23.0(1.29)	0.97
8			Standard+20%	One-way	----	23.7(1.23)	----
9			Standard−20%		----	21.8(1.40)	----
10	WWW	Positive	Standard	One-way	25.9(1.62)	27.3(1.24)	0.95
11		Negative			28.5(3.08)	27.0(1.54)	1.06
12	WBW−E	Positive	Standard	One-way*	31.3(2.21)	45.2(7.52)	0.69
13		Negative			34.2(5.00)	47.5(6.37)	0.72
14	WBW−B	Positive	Standard	One-way	46.8(7.41)	46.1(10.43)	1.02
15		Negative			41.1(6.01)	50.5(8.91)	0.81
16		Positive	Standard+20%		----	46.1(7.32)	----
17			Standrad−20%		----	44.5(8.17)	----
18			Standard	Cyclic loading	46.8(7.41)	44.5(8.32)	1.05
19		Negative			41.1(6.01)	43.7(4.96)	0.94

NOTE*: "One−way" means one−way monotonic loading.

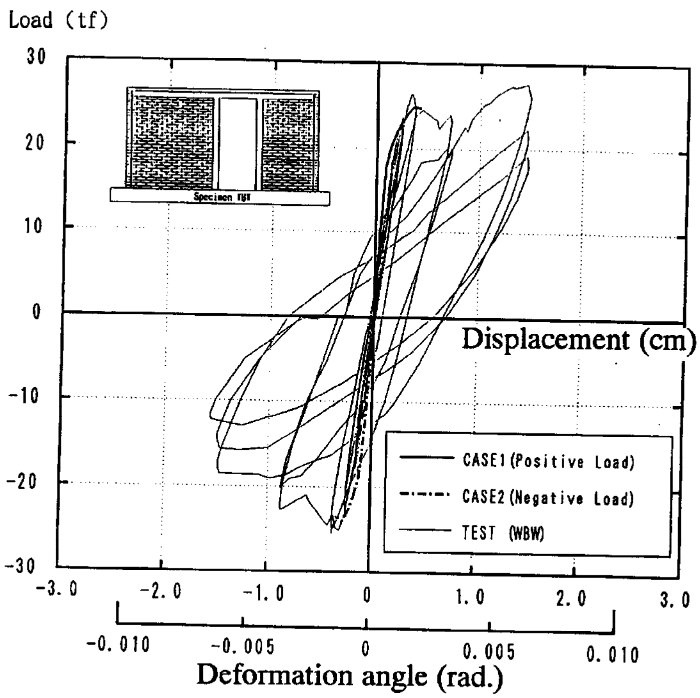

(a) Case 1 and Case 2

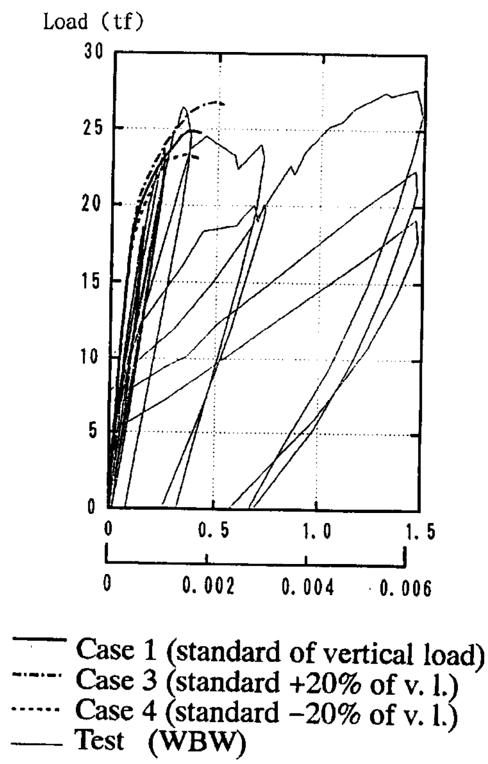

(b) Case 1, Case 3 and Case 4

Fig. 4 A comparison of load−displacement relationships

for investigating the effect of changes of joint status between bricks and concrete, such as opening and slippage, caused by the former loading on the behaviors under loading in the opposite direction.

The effect of the difference in the loading direction for an asymmetric shaped wall can be investigated by comparing Case 1 and Case 2. The effect of the difference in the magnitude of the vertical load can be clarified by comparing Cases 1,3 and 4. A comparison of load−displacement relationships of the test and the anlysis of Case 1 and Case 2 is shown in Fig. 4(a). Although the stiffness is slightly large compared to the test results, Case 1 and Case 2 show good agreement with test results for the strength and displacement at the strength. The effect of the difference in the loading direction can not be found in the analyses expect that Case 1 shows relatively small stiffness in the vicinity of the maximum stress.

Figure 4(b) compares load–displacement relationships of the test and Cases 1,3,and 4 in which the magnitude of the axial load differs from each other. There is no difference in the initial stiffness obtained from the analysis. But the stiffness after the occurrence of cracking (17–18tf) and the strengths are different from each other in the analysis. The strength of Case 1 is 24.8tf, while for Case 3, with the vertical load increased by 20%, the stiffness increased and the strength is 26.8tf (+8%). For Case 4, with the vertical load decreased by 20%, the decline of stiffness occurs a little earlier and the strength is 23.3tf (–6%).

Deformation modes at the maximum load and propagation of cracking are shown in Fig. 5(a) and 5(b) for the test and analysis of Cases 1. The deformation mode obtained from the analysis corresponds well with the test. The cracking process is similar in the four cases of analyses (Case 1 to 4) and it is roughly as follows;
First, shear slip occurred on the boundary surface between the msonry wall and the concrete frame, and successive cracking occurred at the lower corner of the wall.
Cracks developed along the column and the base from the lower corner of the wall.
Cracks progressed in the lower portion of the column, then inclined cracks occurred at the center portion of the wall, first in the wall away from the loading point, and later in the wall close to the loading point.
Inclined cracks progressed in both walls and separation on the boundary surface between the masonry wall and the surrounding frame also progressed, then reached the maximum load.

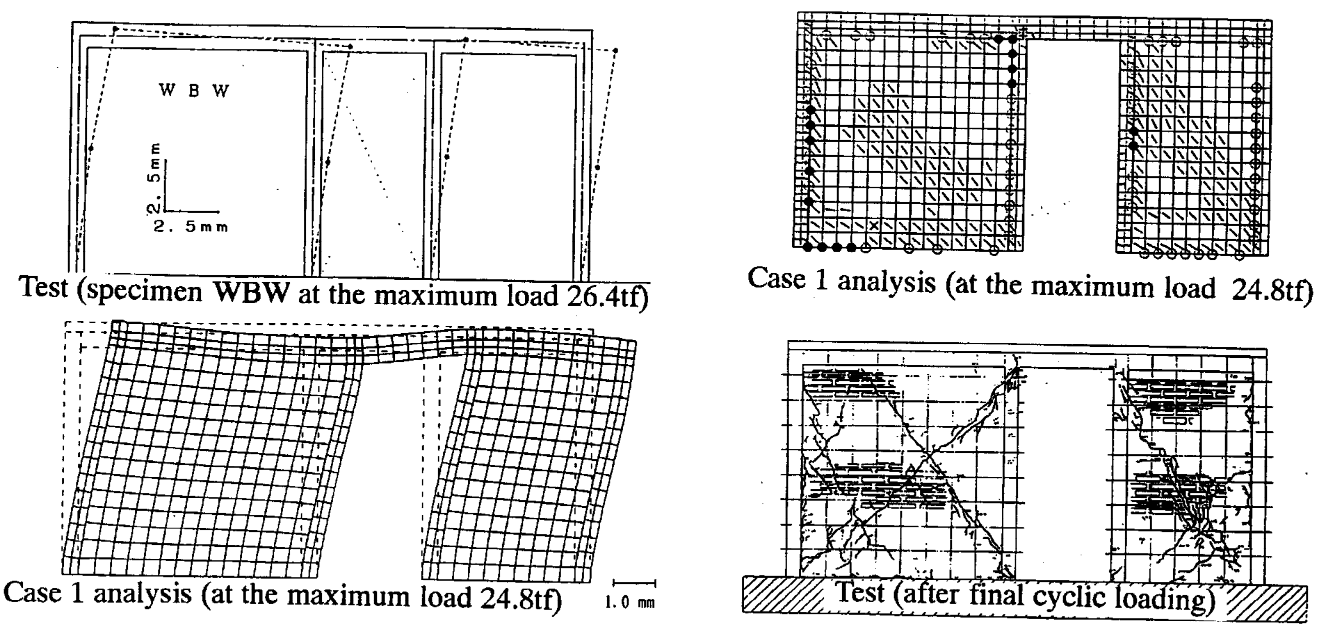

Test (specimen WBW at the maximum load 26.4tf)

Case 1 analysis (at the maximum load 24.8tf)

Case 1 analysis (at the maximum load 24.8tf)

Test (after final cyclic loading)

(a) Deformation mode

(b) Propagation of cracking

Fig. 5 A comparison of deformation and crack of the test with the analysis

By comparing the cracking patterns of Cases 1,3 and 4, it is found that the amount of the vertical load becomes large, progress of cracks is suppressed to some extent. But there is same tendency for cracks to be concentrated in the center of the walls.

Specimen WBW–B corresponds to specimen WBW except horizontal reinforing bars (double deformed bars) in the walls. The effect of the difference in the loading direction for an asymmetric shaped wall can be investigated by comparing Cases 14 and 15. The effect of the difference in the magnitude of the vertical load can be studied by comparing Cases 14, 16 and 17. In order to investigate the effect of the change in status of the boundary between the masonry wall and the concrete frame caused by loading in the opposite direction, a method in which first the load was applied in the opposite direction (20tf), then in the right direction up to the maximum load was used in the analysis of Cases 18 and 19. The breakage of horizontal reinforcing bars was not taken into account in the current analysis, however, it did not seem to be a problem to compare the analytical with the test results because the breakage of reinforcing bars had occurred after a rotation angle of 0.006 rad. in the final cycle and in the vicinity of the maximum load.

A comparison of load–displacement relationships in the test and the anaysis of Cases 14 and 15 is shown in Fig. 6(a). Case 14 closely coincides with the test results on the whole including the maximum load, though the initial stiffness and deflection at the maximum load is slightly larger compared with the test. Case 15 gives good agreement with the initial stiffness of the test, but the maximum load and the deflecting capacity are larger than those of the test. As for the difference in loading directions in the analysis, it becomes clear after a load of 30tf when cracks occurred nearly everywhere in the walls, and negatively loaded Case 15 exhibits higher stiffness and strength than Case 14. There is a tendency that the larger the magnitude of the vertical load becomes, the higher the stiffness and the strength are.

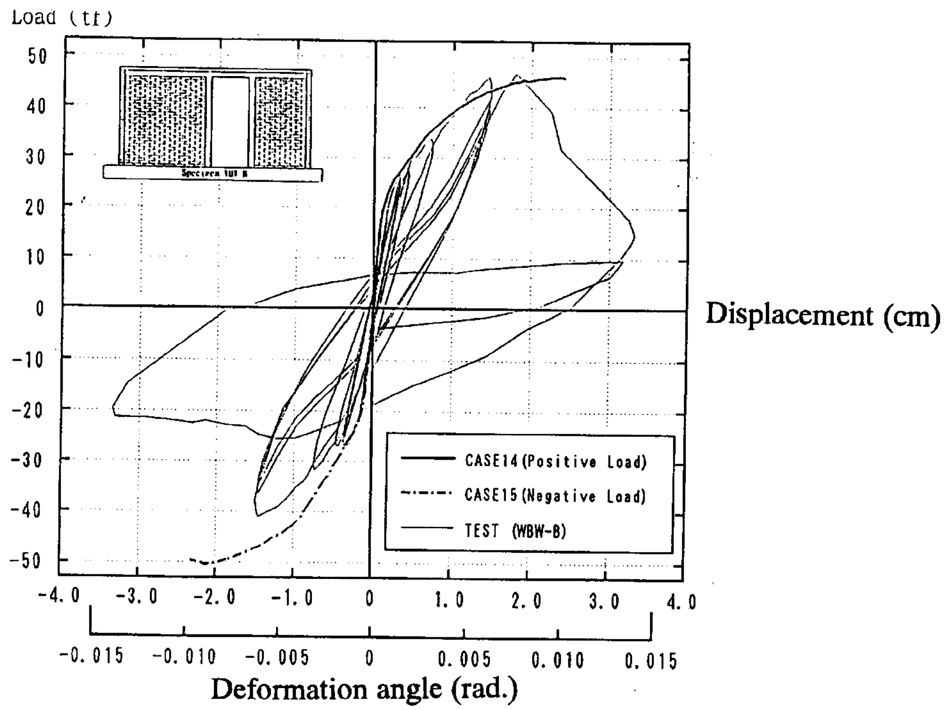

(a) Case 14 and Case 15

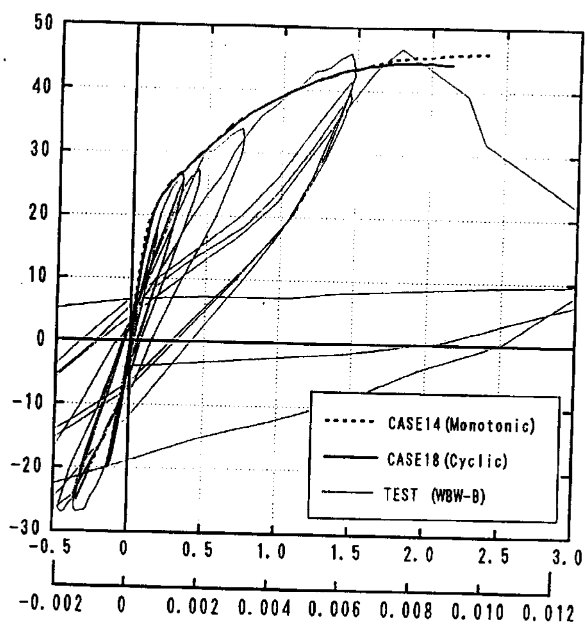

(b) Case 14 and Case 18

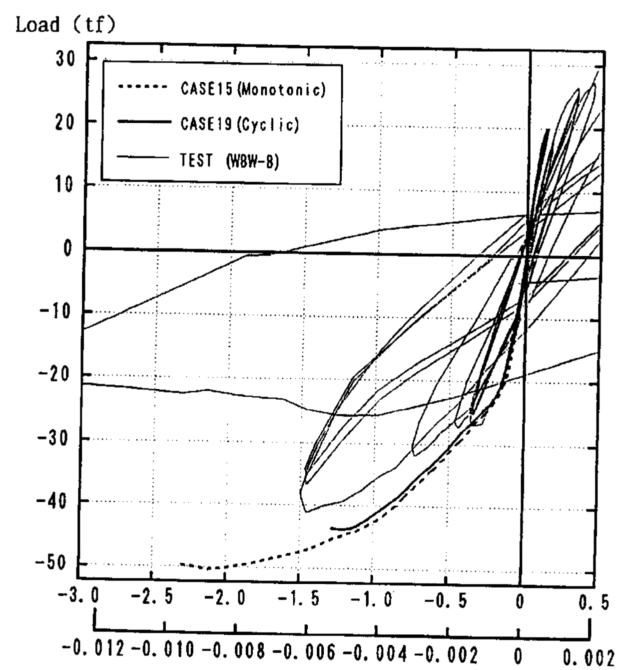

(c) Case 15 and Case 19

Fig. 6 A comparison of load–displacement relationships in the cases of specimen WBW–B having horizontal reinforcements

Figure 6(b) compares load–displacement relationships of the test and Cases 14 and 18 in which the loading methods differ from each other. The loop for loading and unloading in the negative direction of Case 18 agrees with the test results. After that the analytical results under positive loading shows slightly smaller stiffness and strength compared with Case 14 which was applied monotonic loading.

Figure 6(c) compares load–displacement relationships of the test and Cases 15 and 19 in which the loading methods is different from each other, as well. As mentioned before, cracks occurred in the center of the walls of the specimen which did not have horizontal reinforcing bars, however, cracks occurred all over the walls in both the test and the analysis of specimen WBW–B.

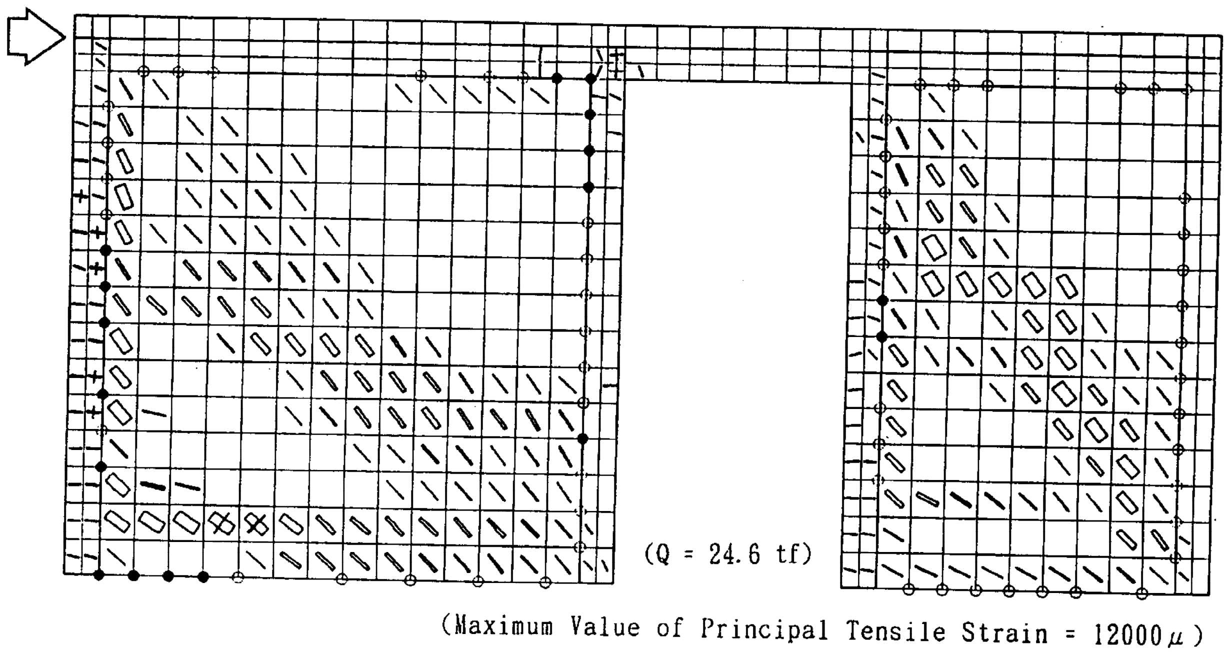

(a) Analysis Case 1 for specimen WBW having no horizontal reinforcements

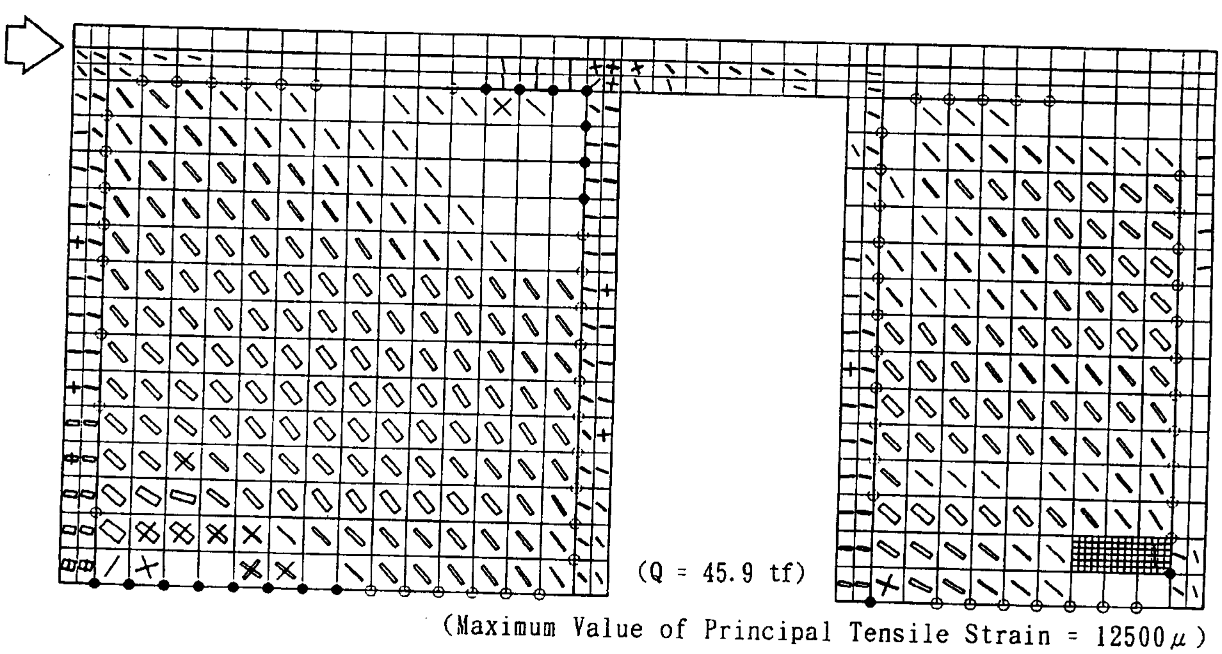

(b) Analysis Case 14 for specimen WBW–B having horizontal reinforcements

small crack width
large crack width
slip more than 0.1 mm
separation at boundary
compressive strain softening
compressive failure

Fig. 7 A comparison of crack pattern of masonry brick wall

In order to compare the difference in crack propagations, cracking patterns of Case 1 for specimen WBW and Case 14 for specimen WBW–B are shown in Fig. 7. The relative magnitude of the principal tensile strain of cracked elements in the figures is indicated, that is, cracks drawn close to a line indicate small opening and cracks drawn in a wide rectangular shape indicate large opening. It can be seen that cracks are predominant diagonally in the center of the walls in Case 1, while in Case 14, cracks spread all over the walls. Strain softening and crushing of concrete occurred in the wall near the maximum load.

CONCLUSION

The following conclusion have been obtained from the results of nineteen cases of analyses for five confined masonry wall specimens having different shapes and different reinforcing conditions with major parameters being the loading direction and the magnitude of vertical load.
1)The test results are simulated well by the analyses in which the reinfored concrete frame and the masonry wall are connected by linkage elements consisting of two ortohogonal springs. The characteristics of the spring in the shear direction is varied as a function of the compression force acting in the spring in the normal direction.
2)It has been confirmed that the proposed analytical method is applicable to specimens with different shaped wall, reinforcing conditions and loading directions.
3)The difference in the vertical load has an effect on the stiffness and the strength. But the effect is not remarkable if the vertical load changes within ±20% of the standard value, and the increase of the strength is 8% at the most when the vertical load increases by 20% of the standard value.
4)The strength was overestimated by the analysis for the specimen in which reinforcing bars had been broken at welding portions during the early stages of the test, because breakage of reinforcing bars was not taken into account in the analysis.
5)The stiffness and the strength obtained from the analysis previously loaded one cycle in the opposite direction were slightly less than those from the monotonic loading analysis.

ACKNOWLEDGMENT

This study was part of the cooperation program to Mexico by Japan International Cooperation Agency (JICA). Dr. Roberto Meli, Dr. Sergio M. Alcocer, Mr. Lorenzo Sanchez, Mr. Tomas Sanchez, Mr. Pablo Olmos, Mr. Fermin Leon, Mr. Heraldo Aguilar and Mr. Jose Antonio Zepeda of CENAPRED; assisted in the testing itself and supplied variable test results. Mr. Motoji Saito, Mr. Mitsuo Yoshida, Dr. Koji Yoshimura and Miss Mie Tanaka kindly allowed the authors to use their research, for example, the results of material tests, translation of the Mexican building code, and so on. The authors would like to express their gratitude for the contributins by the people mentioned herein.

REFERENCES

Darwin, D. and D.A. Pecknold (1977). Nonlinear Biaxial Stress–Strain Law for Conrete. **J. of the Engineering Mechanics Division, ASCE, Vol.103**, NO.EM2, pp.229–241.
Fafitis, A. and S.P. Shah (1985). Lateral Reinforcement for High–Strength Concrete Columns, **ACI S.P., No.SP–87**, pp.213–232.
Fujii, K., T. Kubo, H. Katsumata, *et al.* (1990). Evaluation of Seismic Capacity and Retrofit of an Existing Brick Masonry Structure (Part 1 to 4). **Proc. of Annual Conv., Struct. 2, AIJ**, pp.1009–1016. (in Japanese).
Ishibashi, K., R. Meli, S.M. Alcocer, F. Leon and T.A. Sanchez (1992). Exerimental Study on Earthquake–Resistance Design of Confined Masonry Structures. **Proc. of 10WCEE, Vol.6**, pp.3469–3474.
Kupfer, H.B. and K.H. Gerstle (1973). Behavior of Concrete under Biaxial Stress. **J. of the Engineering Mechanics Division, ASCE, Vol.99, No.EM4**, pp.835–866.